J Mol Model (2011) 17:2751–2758
DOI 10.1007/s00894-011-0967-x

ORIGINAL PAPER

Initial reactions of methyl-nitramine confined inside armchair (5,5) single-walled carbon nanotube

Luoxin Wang · Changhai Yi · Hantao Zou · Houlei Gan · Jie Xu · Weilin Xu

Received: 25 November 2010 / Accepted: 10 January 2011 / Published online: 29 January 2011

Abstract The dissociation and isomerization reactions of methyl-nitramine(MNA) confined inside armchair CNT (5,5) single-walled carbon nanotube were investigated by using the ONIOM (B3LYP/6-311++G**:UFF) method. The results showed that some geometries of the confined MNA were modified by the CNT(5,5) in comparison with the structure of the isolated MNA. By analyzing the relevant structures and energies involved in the dissociation and isomerization reactions, we found that the transition state structures of the isomerization reactions to form CH_3NHONO (R1) and CH_3NNOOH (R2) were modified by the confinement of CNT(5,5). However, this confinement does not evidently affect the transition state structure of the HONO elimination reaction (R3). In addition, no transition state was found for the N-N bond dissociation (R4) of the isolated MNA, but this dissociation process occurred via a transition state for the confined MNA. When MNA was confined inside CNT(5,5), the activation energies of R1, R2, and R4 were decreased obviously but the energy barrier of R3 was increased slightly. The order of activation energy for these four initial reactions was also changed by the confinement of CNT(5,5). Furthermore, it was found that the relative energies of the intermediates formed by the isomerization and dissociation of MNA were also modified by the confinement of CNT(5,5). These intermediates become more stable in the confined case than in the isolated case. It was concluded that the initial reactions of MNA could be modified evdiently by confinement within a carbon nanotube.

L. Wang · C. Yi · H. Zou · H. Gan · J. Xu · W. Xu (✉)
Key Laboratory of Green Processing and Functional Textiles of New Textile Materials, Ministry of Education, Wuhan Textile University,
No. 1 Fangzhi Road, Luxiang,
Wuhan 430073, People's Republic of China
e-mail: weilin_xu@wtu.edu.cn

Keywords *Ab initio* · Carbon nanotube · Confinement effect · Dissociation · Isomerization · Methyl-nitramine

Introduction

Carbon nanotubes (CNT) have a unique one dimensional nano-cavity. The material inserted into the nano-channel shows some interesting physi-chemical properties due to the confinement effect of the nanotube. For example, Bao et al. [1] found that the Fe_2O_3 nano-particles filled into the carbon nanotube can be easily reduced to iron particles. Some metal nano-particles show fascinating catalytic action when they are encapsulated into the nanotubes [2, 3]. The molecular dynamics simulations have predicted the formation of a strongly connected one-dimensional water wire in a narrow single-walled carbon nanotube (SWNT). An ice-like water structure can be formed inside a SWNT with a larger radius [4, 5]. A vibrational spectroscopy study has manifested that the water phase inside SWNT has an unusual form of hydrogen-bonding due to the confinement [6]. Additionally, it has been found experimentally that the water confined in channels of SWNTs can be directly split by visible light [7]. All the above illustrate that CNT can modify the reactivity of the confined materials.

The application of CNT in the field of energetic materials has also attracted great attention. Embedding of energetic materials into CNTs to form energetic nano-composition is a current hot topic. Polymeric nitrogen or polynitrogen, as an extremely powerful high-energy-density material (HEDM), only exists under the very extreme conditions (high pressure and temperature), which heavily hinders its practical application in explosive or propellant. Theoretical study has predicted that a polymeric nitrogen chain (N_8) encapsulated in a SWCNT exhibits good

stability at ambient pressure and room temperature [8, 9]. The confinement of CNT favors the stability of the N_8 chain. However, it is not clear whether the stability of other energetic materials might be improved when they are filled into CNTs. Nitromethane is one of the energetic compounds with the simplest molecular structure. Recently, on the basis of calculations, we found that the decomposition activation energy of nitromethane was reduced evdiently by confinement within a carbon nanotube with a small diameter, but the activation energy was not modified by the CNTs with the larger radius. The chirality of a carbon nanotube shows no effect [10]. Furthermore, we found that the rearrangement of nitromethane was evidently modified by the confinement within a CNT(5,5) [11]. The current investigations suggest that different energetic compounds will show different chemical activity when they are confined inside CNT.

Nitramine explosives are one of the most commonly used classes of energetic materials. It would be very interesting to prepare the energetic nano-composites by filling this kind of explosives into a CNT. Methyl-nitramine (MNA) is a prototypical energetic nitramine compound. The thermal decomposition and isomerization mechanism of MNA have been studied intensively by both experimentalists and theoreticians. The following equations (R1-R4) present the possible paths for the initial reaction of MNA. Wei et al. [12] investigated the competitive relationship of these four routes with high level theoretical calculations. They believed that MNA isomerization to $CH_2NHNOOH$ (R2) is the dominant reaction under low temperature. The N-N bond dissociation (R4) and isomerization to CH_3NHONO (R1) will compete with R2 under high temperature. Experimentally, Kekin et al. [13] also inferred that the thermal decomposition of MNA mainly involves the dissociation of the N-N bond at high temperature.

$$CH_3NHNO_2 \rightarrow CH_3NHONO \quad (R1)$$

$$CH_3NHNO_2 \rightarrow CH_2NHNOOH \quad (R2)$$

$$CH_3NHNO_2 \rightarrow CH_2NH + HONO \quad (R3)$$

$$CH_3NHNO_2 \rightarrow \cdot NHCH + \cdot NO_2 \quad (R4)$$

So far, there is no report on the thermal decomposition and isomerization of MNA confined inside a CNT. In this study, we chose an armchair SWCNT as the model tube. Using ONIOM method, we calculated the molecular structure and initial reaction of MA confined inside CNT and explored the confinement effect of CNT on the thermal decomposition and isomerization of MNA. It is well-known that these initial reactions of nitramines are responsible for their safety, sensitivity, and explosive properties. Therefore, to study the structure and initial reaction of the energetic nitramines embedded inside CNT can strengthen the understanding of nitramine-CNT interaction and provide the theoretical guide for the design of CNT-based energetic materials.

Computational details

In order to achieve reasonable accuracy and save computational cost, the ONIOM [14] method has been widely applied in the large-scale quantum chemical molecular system. The studied molecular system can be divided into two or three layers which are treated with different theoretical models in the ONIOM calculation. Here, the complex formed by the MNA being embedded inside the CNT was divided into two layers. The high layer included the MNA, which was described with the hybrid B3LYP [15] approach in conjunction with the 6-311++G** basis set. The lower layer comprised the CNT, which was treated with the universal force field (UFF) [16]. The combination of density functional theory (DFT) with UFF molecular mechanics has been successfully applied to the modeling of the noncovalent interactions between CNT and some small molecules (e.g. O_2, methanol, and ethanol, etc.) [17–20].

The single-walled armchair CNT(5,5) was chosen as the model tube. The hydrogen atoms were added at the open ends of the tube to avoid dangling bonds. The complex formed by MNA and CNT(5,5) is labeled as MNA@CNT(5,5). The other complexes are labeled the same way. Considering the biradical character of MNA during the N-N bond dissociation, we used ONIOM(UB3LYP/6-311++G***:UFF) method with the keyword guess=(mix, always) [21–24] to scan the potential energy curve and optimize the transition state. Table 1 presents the relevant energies of all species. All the calculations were performed using Gaussian 03 program package [25].

Results and discussion

Molecular structure and adsorption energy for the confined MNA

Figure 1 gives the molecular structures of the MNA@CNT (5,5) and the isolated MNA. The geometrical parameters of the isolated MNA optimized at the B3LYP/6-311++G** level of theory are consistent with the values reported in ref. [12]. It can be seen from Fig. 1 that the molecular structure of MNA is influenced by the confinement of CNT(5,5). For

Table 1 The total energies and relative energies for all the important species discussed in the text

Species	Total energy (a.u.)	ZPE (kJ mol^{-1})	Relative energy (kJ mol^{-1})	Imaginary frequency (cm^{-1})
CNT(5,5) [a]	3.36159	4883.8	-	-
MNA	-300.44509	176.0	0 [b]	-
CH_3NHONO	-300.40536	168.7	97.0 [b]	-
CH_3NNOOH	-300.43076	173.4	35.0 [b]	-
(CH_2NH+HONO)	-300.45055	163.7	-26.6 [b]	-
($\cdot NHCH_3$+$\cdot NO_2$)	-	-	~205 [b]	-
TS_1	-300.32247	155.2	301.1 [b]	-502.2
TS_2	-300.38299	161.0	148.0 [b]	-1908.5
TS_3	-300.36548	156.4	189.4 [b]	-1439.6
MNA@CNT(5,5)	-297.09228	5074.4	0 [c]	-
CH_3NHONO@CNT(5,5)	-297.08862	5060.2	-4.6 [c]	-
CH_3NNOOH@CNT(5,5)	-297.09021	5066.2	-2.8 [c]	-
(CH_2NH+HONO)@CNT(5,5)	-297.15083	5050.4	-177.7 [c]	-
($\cdot NHCH_3$+$\cdot NO_2$)@CNT(5,5)	-297.07015	5040.5	24.2 [c]	-
TS_1@CNT(5,5)	-296.98757	5047.6	248.1 [c]	-413.6
TS_2@CNT(5,5)	-297.03746	5056.4	125.9 [c]	-1897.4
TS_3@CNT(5,5)	-297.00923	5054.5	198.2 [c]	-1364.7
TS_4@CNT(5,5)	-297.02493	5057.1	159.5 [c]	-279.8

[a] calculated at the UFF force field

[b] relative to the energy of MNA, calculated at the B3LYP/6-311++G** level of theory

[c] relative to the energy of MNA@CNT(5,5), calculated at the ONIOM(B3LYP/6-311++G**:UFF) level of theory

example, the N-N and C-N bond lengths of the confined MNA are decreased by about 0.01and 0.018 Å. The ONO bond angle is stressed by 1.8° and the CNN bond angle changes from 118.2° to 124.7°. The nitro group rotates around N-N bond to some extent.

For the MNA@CNT(5,5), the adsorption energy is calculated as $E_{adsorp}=E_{MNA@CNT(5,5)} - E_{MNA} - E_{CNT(5,5)}$. We found that this energy was calculated to be about -8.5 kJ mol^{-1}. This means that the embedding of MNA within CNT(5,5) favors in energy.

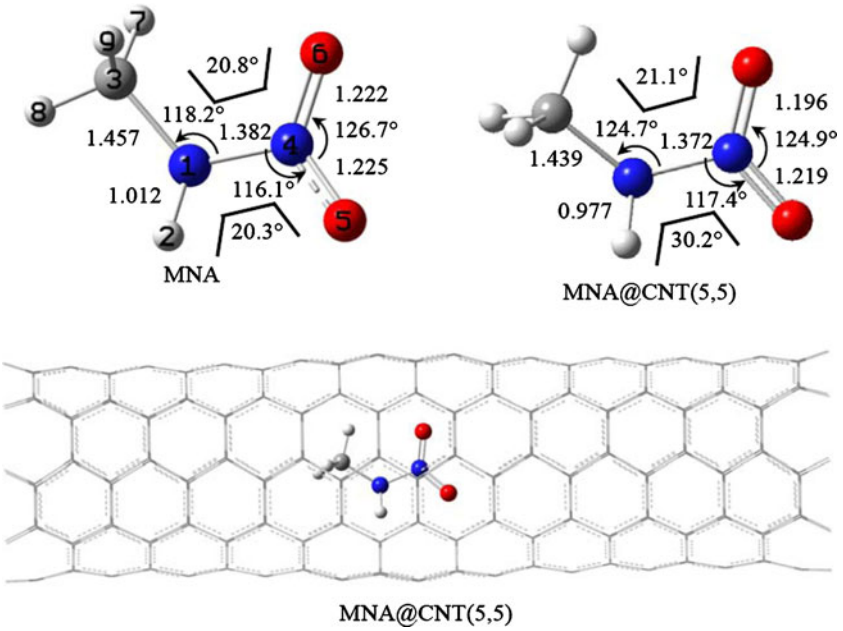

Fig. 1 Molecular structures of MNA and MNA@CNT(5,5), all bond lengths are in angstroms, and bond angles and dihedral angles are in degree

CH_3NHNO_2 isomerization to CH_3NHONO (R1)

The nitro-nitrite isomerization is considered as one of the important initial reactions for the thermal decomposition of nitramine compounds [26, 27]. Using B3LYP/6-311++G** and ONIOM(B3LYP/6-311++G**:UFF) levels of theory, we optimized the transition states of this isomerization reaction for the isolated MNA and confined one, respectively. Figure 2 gives the two transition states which are labeled as TS_1 and TS_1@CNT(5,5). TS_1 has an imaginary frequency of 502.3 cm^{-1} and TS_1@CNT(5,5) has an imaginary frequency of 413.6 cm^{-1}. Intrinsic reaction coordinate (IRC) calculations were further performed to verify the two transition states.

As can be seen from Fig. 2, the N-N bond length of the TS_1@CNT(5,5) is shorter by 0.016 Å than that of TS_1. That is to say, the N-N bond vibration of the confined MNA is not as intensive as that of the isolated one when the nitro-nitrite isomerization of MNA occurs. This indicates that the activation energy of TS_1@CNT(5,5) should be lower than that of TS_1. In addition, the CNN bond angle becomes more extended so that the MNA can adapt the cavity of CNT(5,5).

In Table 1, we can see that the energy of TS_1 is 301.1 kJ mol^{-1} in comparison with that of the isolated MNA, calculated at the B3LYP/6-311++G** level of theory. With respect to MNA@CNT(5,5), TS_1@CNT(5,5) was found to have the activation energy of 248.1 kJ mol^{-1}, about 53.0 kJ mol^{-1} lower than the activation energy of TS_1. This means that the confinement of CNT(5,5) can favor the CH_3NHNO_2 isomerization to CH_3NHONO.

The confinement of CNT(5,5) also has great effect on the relative energy of the nitrite product. In the case of an isolated state, the relative energy of CH_3NHONO with respect to MNA is 97.0 kJ mol^{-1}. In the case of a confined state, however, the energy of CH_3NHONO@CNT(5,5) is found to be lower by 4.6 kJ mol^{-1} than that of MNA@CNT (5,5), which suggests that the CH_3NHONO is more stable than MNA when they are confined inside CNT(5,5).

CH_3NHNO_2 isomerization to CH_3NNOOH (R2)

The isomerization from MNA to CH_3NNOOH is indeed an intramolecular H-migration from a nitrogen to an oxygen atom. In the present stage, the investigation on this H-migration of MNA is rarely reported in literature from the point of view of the theoretical calculation. Experimentally, it has been suggested that the 1,3-hydrogen shift is a rate-determining step for the catalyzed decomposition of nitramide (NH_2NO_2) [28, 29]. On the basis of the B3LYP/6-311++G** and ONIOM(B3LYP/6-311++G**:UFF) calculation, the transition states of the isomerization from MNA to CH_3NNOOH for the isolated MNA and confined one were obtained, which are labeled as TS_2 and TS_2@CNT(5,5), repectively. Figure 3 gives their geometrical parameters. TS_2 and TS_2@CNT(5,5) have only one imaginary frequency (1908.5 and 1897.4 cm^{-1}). It can be seen that the N-H and O-H bond lengths of TS_2 are 1.298 and 1.312 Å. The corresponding N-H and O-H bond lengths of TS_2@CNT (5,5) are 1.265 and 1.261 Å, respectively. Therefore, the distance of H-migration is decreased by the confinement of CNT(5,5) when MNA isomerizes to CH_3NNOOH.

In view of the energy, with respect to MNA, TS_2 has an energy barrier of about 148.0 kJ mol^{-1}. The activation energy of TS_2@CNT(5,5) was calculated to be about 125.9 kJ mol^{-1} relative to the energy of MNA@CNT(5,5). Compared with the isolated state, the activation energy of the R2 reaction is lowered by about 22.1 kJ mol^{-1} under the

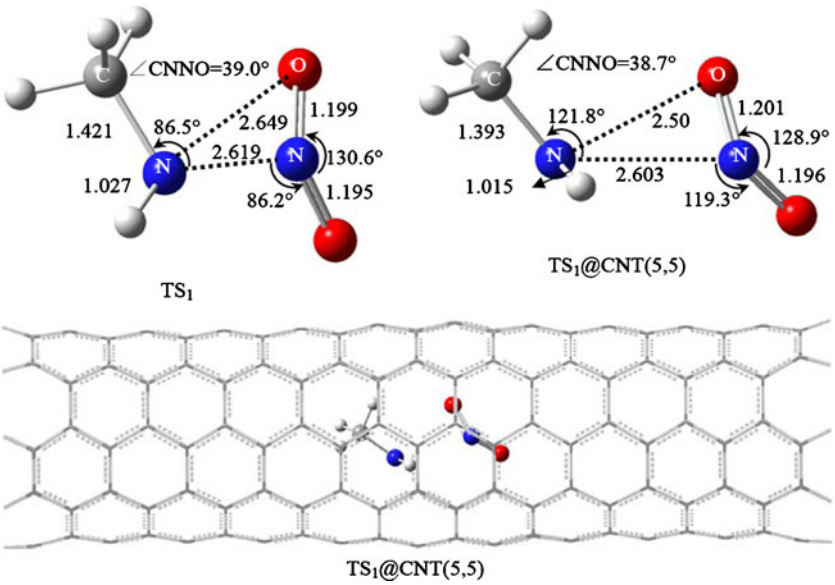

Fig. 2 Molecular structures of the transition states for the nitro-nitrite isomerization reaction of the isolated MNA and MNA@CNT(5,5). Bond lengths, bond angles and dihedrals are illuminated as in Fig. 1

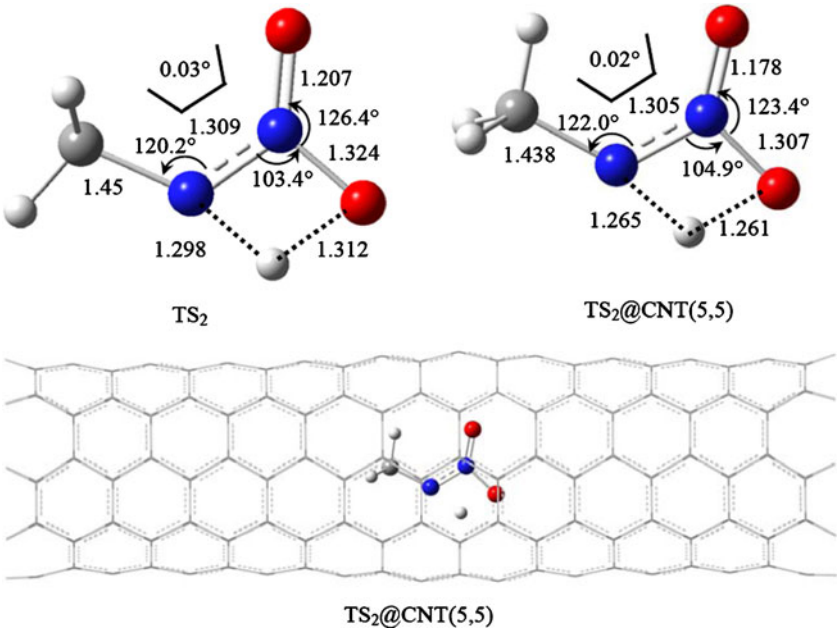

Fig. 3 Molecular structures of the transition states for the H-migration isomerization reaction of the isolated MNA and MNA@CNT(5,5). Bond lengths, bond angles and dihedrals are illuminated as in Fig. 1

confined state. Namely, the confinement of CNT(5,5) also facilitates the isomerization form MNA to CH_3NNOOH. Additionally, CH_3NNOOH becomes more stable under the confined state because the energy of CH_3NNOOH@CNT (5,5) was calculated to be lower by about 2.8 kJ mol^{-1} than that of MNA@CNT(5,5). Under the isolated state, the energy of CH_3NNOOH is higher by 35.0 kJ mol^{-1} than that of MNA.

Elimination of HONO (R3)

As for the representative nitramine explosives (e.g. dimethylnitramine, hexahydro–1,3,5–trinitro–1,3,5–triazine, octahydro-1,3,5,7-tetranitro-1,3,5,7-tetrazocine, etc), some theoretical studies have shown that the elimination of HONO is one of the important initial reactions. The activation energy of R3 is closer to that of the loss of the NO_2 group [30–32]. Figure 4 gives the transition states of the HONO elimination of MNA in the isolated and confined states, which are referred to as TS_3 and TS_3@CNT(5,5). Only one imaginary frequency was found for each transition state. The transition states in both states are formed by the migration of H-atom from the CH_2 to the NO_2 group and the elongation of the N-N bond. Examining the two transition states, it can be found that the structures of MNA are very similar to each other. Furthermore, the activation energies of the two transition states are also found to be very close. The difference in energy between them is only about 8.8 kJ mol^{-1}. This

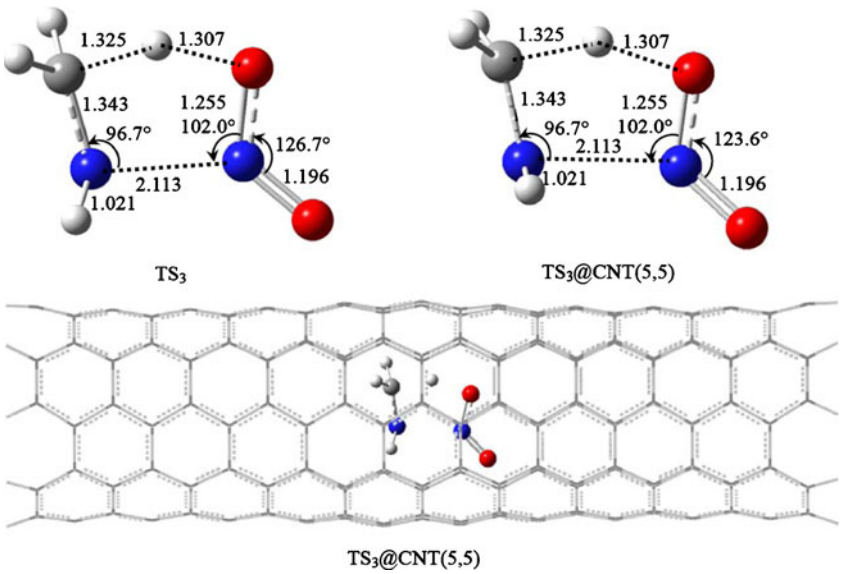

Fig. 4 Molecular structures of the transition states for the HONO elimination reaction of the isolated MNA and MNA@CNT(5,5). Bond lengths, bond angles and dihedrals are illuminated as in Fig. 1

means that the HONO elimination of MNA is not affected obviously by the confinement of CNT(5,5). Nevertheless, it can be found from Table 1 that the confinement effect has great influence on the product of HONO elimination. The energy of complex (CH_2NH+HONO) is calculated to be 22.6 kJ mol^{-1} lower than that of MNA in the isolated state, but the energy of (CH_2NH+HONO)@CNT(5,5) is lower by about 177.7 kJ mol^{-1} than that of MNA@CNT(5,5).

N—NO_2 bond dissociation (R4)

Many experimental and theoretical investigations have manifested that the N-NO_2 dissociation leading to biradicals determines the decomposition and explosion of nitramine compounds [32–34]. To explore the N-NO_2 dissociation of MNA, we calculated the potential energy curve by scanning the N-NO_2 bond at the UB3LYP/6-311++G** level of theory. It can be seen that from the potential energy curve, shown in Fig. 5, no transition state exists on this curve. The dissociation limit is expected to be about 205 kJ mol^{-1} from the potential energy curve, which is slightly higher than the N-NO_2 bond dissociation energy (186.8~188.5 kJ mol^{-1}) reported by Wei et al. [12].

Figure 5 also provides the potential energy curve of N-NO_2 rupture when MNA is confined inside CNT(5,5), which is calculated at the ONIOM(UB3LYP/6-311++G**: UFF) level of theory. In this case, the potential energy curve is evidently different from that in the isolated state. A maximum point exists on the potential energy curve of MNA@CNT(5,5), indicating that a transition state should be taken into account. This transition state, labeled as TS_4@CNT(5,5) was further optimized, the geometries of which are given in Fig. 6. IRC was performed to confirm this transition state connecting the MNA and the product of N-NO_2 bond dissociation. Only one imaginary frequency of 279.8 cm^{-1} was found. Both R1 and R4 reaction under the confined state involve the evident elongation of N-N bond, but the structures of the corresponding transition states are obviously different. The N-N bond length is stretched to 2.619 Å in TS_1@CNT(5,5), but this bond length is extended to 2.218 Å in TS_4@CNT(5,5) in comparison with the structure of MMA@CNT(5,5).

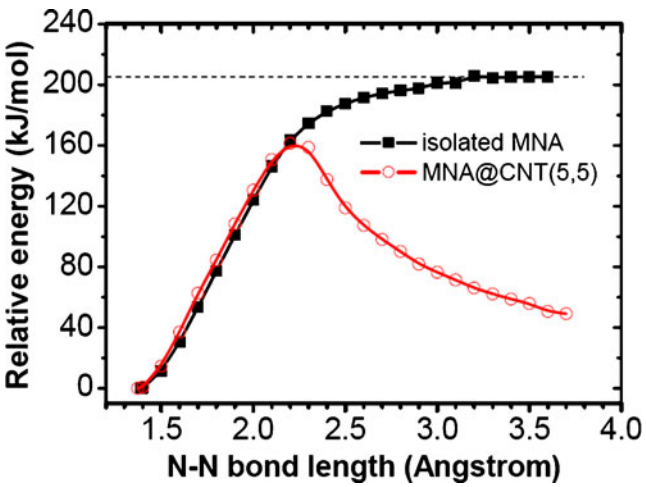

Fig. 5 Potential energy curves of the isolated MNA and MNA@CNT (5,5) along the N-NO_2 bond length

The energy barrier of TS_4@CNT(5,5) was calculated to be about 159.5 kJ mol^{-1} (see Table 1) with the inclusion of zero-point energy correction, about 45.5 kJ mol^{-1} lower than the N-NO_2 dissociation limit. The N-N bond homolytic rupture of the confined MNA has a lower activation energy than that of the isolated MNA. Therefore, it can be concluded that the confinement of NCT(5,5) can obviously promote the N-NO_2 dissociation of MNA.

Analysis of the potential energy surface

Figure 7 presents the potential energy surface (PES) of the dissociation and isomerization reactions for both the isolated MNA and the MNA@CNT(5,5). In view of the energy, MNA isomerization to CH_3NNOOH has the lowest activation energy among these initial steps of the isolated MNA. Namely, R2 is the most favorable pathway in energy. This is consistent with the PES calculated by Wei et al. [12]

With respect to the isolated state, the PES of MNA in the confined state changes very obviously. Due to the confinement of CNT(5,5), the activation energies of R1,R2 and R4 are lowered by 53.0, 22.1, and 45.5 kJ mol^{-1}, respectively, but the energy barrier of R3 is increased by 8.8 kJ mol^{-1}. What is more, the order of activation energy for these initial reactions is also affected by the confinement effect. For the isolated MNA, the order is R1>R4>R3>R2. For the confined MNA, the order is R1>R3>R4>R2. In both cases, the nitro-nitate rearrangement (R1) is the most unfavorable pathway in energy and the isomerization to CH_3NNOOH (R2) has the lowest activation energy. It is also shown from Fig. 7 that the relative energies of the intermediates originating from the isomerization and dissociation of MNA are evidently modified by the confinement of CNT (5,5). In the cavity of CNT(5,5), these intermediates have lower energies and become more stable with respect to the corresponding unconfined ones.

Hall et al. [35, 36] have calculated the Menshutkin S_N2 reaction inside SWCNT. They found that the activation energy of H_3N+H_3CCl is lowered inside the CNT(8,0) and CNT(9,0) with respect to the energy barrier in the gas state. However, the activation energy of Cl+H_3CCl was found to be increased by the confinement of CNT(6,6). They attributed the changing in activation energy of S_N2 reaction to the "solid solvent" effect of CNT. That is, the SWNTs are expected to have greater longitudinal polarizability,

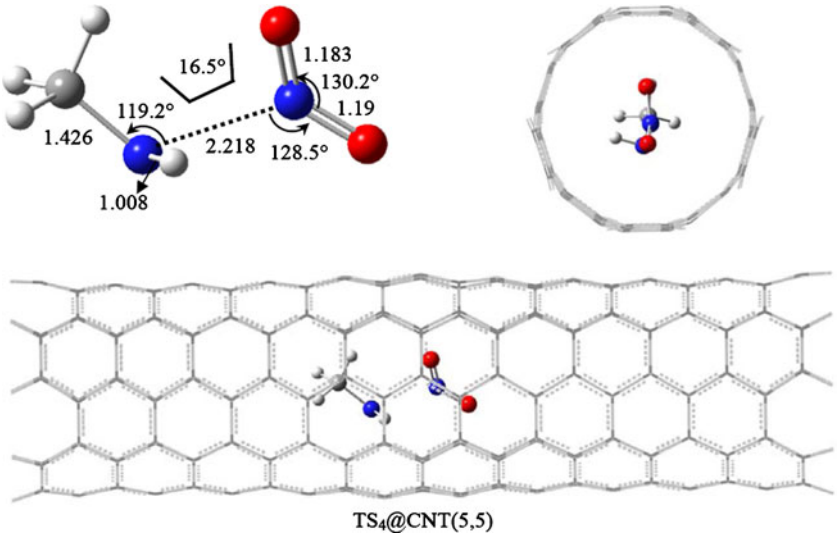

Fig. 6 Transition state of MNA@CNT(5,5) during the N-NO_2 bond dissociation. Bond lengths, bond angles and dihedrals are illuminated as in Fig. 1

which has a great effect on the reaction involving the polar molecules with axial symmetry. Additionally, on the basis of the DFT calculation, Xiao et al. [37] found that the [2+2] cycloaddition reaction between CH_2O and PH_3CH_2 was not influenced by the SWCNT. They explained it as that while taking the linear arrangement for S_N2 reaction, the reactants do not possess the axial symmetry for the studied [2+2] cycloaddition reaction.

The "solid solvent" effect can be used to partially explain the effect of CNT(5,5) on the dissociation and isomerization of MNA. From our calculations, however, the different initial reactions of MNA are modified differently by the confinement of CNT(5,5). That is, it is not enough to state the confinement effect only in view of the axial symmetry of reactants inside CNT. Therefore, considering the unique properties of CNT, we can not exclude the possibility that the other factors, such as the electron deficiency of the interior CNT surface and the weak interaction between reactants and CNT, etc., could also have an effect on the dissociation and isomerization reactions of MNA. More rigorous theoretical studies are needed to shed light on these factors.

In the present stage, there are still some ambiguous questions about the energetic compounds inside CNT. For example, the characteristics of CNT are dependent on the tube diameter and chirality. It is unclear how the size and chirality of CNT affect the isomerization and dissociation of confined MNA. In addition, the carbon nanotubes are often imperfect and contain various defects no matter what method is applied to generate tubes. It would also be very interesting to explore the effect of the CNT with defects on the energetic compounds. Finally, we also hope that in the near future

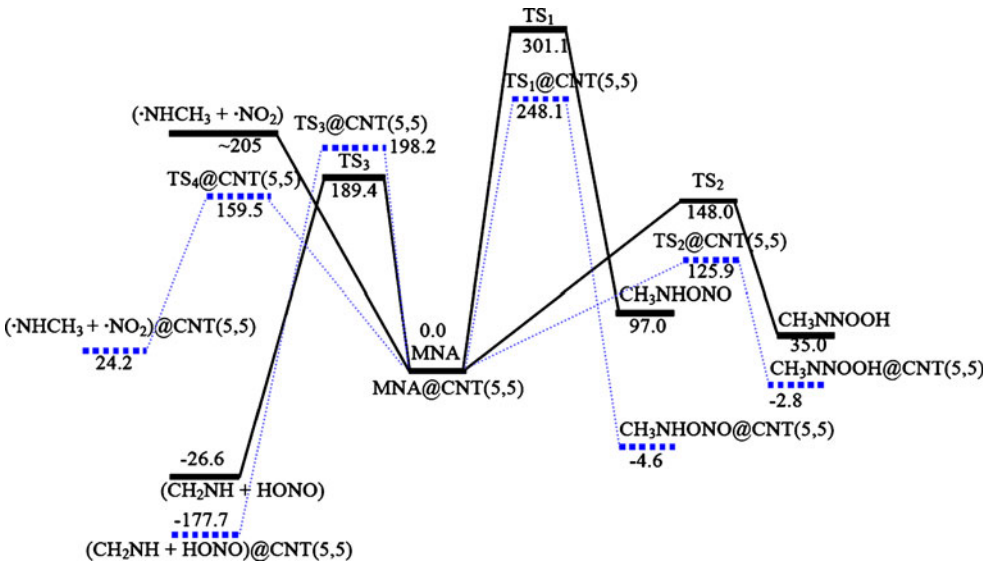

Fig. 7 Potential energy surface of the isomerization and dissociation pathways for the isolated MNA (solid line) and MNA@CNT(5,5) (dashed line). Relative energies are given in kJ mol^{-1}

experimental evidence will clarify the reaction of energetic compounds confined inside CNTs.

Conclusions

The ONIOM (B3LYP/6-311++G**:UFF) calculations showed that the geometry and chemical activity of MNA was changed when it was confined inside CNT(5,5). With respect to the isolated state, the N-N and C-N bond lengths of MNA in the confined state were shortened obviously and the CNN bond angle was increased. The nitro group rotated around the N-N bond to some extent. It was found that the transition state structures of the CNT-confined MNA isomerizing to CH_3NHONO (R1) and CH_3NNOOH (R2) were different from those of the isolated MNA. However, the confinement of CNT(5,5) had little influence on the transition state structure of the HONO elimination reaction (R3). Furthermore, we found that there was no transition state for the N-N bond dissociation (R4) of the isolated MNA, but this dissociation process needs to overcome a transition state for the CNT-confined MNA. The activation energies of R1, R2, and R4 were decreased obviously and the energy barrier of R3 was increased slightly due to the confinement of CNT(5,5). The order of activation energy for these four initial reactions was also modified by the confinement within a CNT(5,5). In both the confined and isolated states, the R1 reaction is the most unfavorable pathway in energy and the R2 has the lowest activation energy. Additionally, we found that the confinement of CNT(5,5) also caused significant decreasing in the energies of the intermediates produced by the initial reactions of MNA. These intermediates should be more stable in the confined case than in the isolated case.

Acknowledgments This research was supported by the Key Project of Chinese Ministry of Education (Grant No. 209080) and the Research Foundation of Education Bureau of Hubei Province, China (Grant No. Z20101601).

References

1. Chen W, Pan X, Willinger MG, Su DS, Bao X (2006) J Am Chem Soc 128:3136–3137
2. Pan X, Fan Z, Chen W, Ding Y, Luo H, Bao X (2007) Nat Mater 6:507–511
3. Chen W, Fan Z, Pan X, Bao X (2008) J Am Chem Soc 130:9414–9419
4. Mann DJ, Halls MD (2003) Phys Rev Lett 90:195503(4)
5. Wang J, Zhu Y, Zhou J, Lu XH (2004) Phys Chem Chem Phys 6:829–835
6. Byl O, Liu JC, Wang Y, Yim WL, Johnson JK, Jr JTY (2006). J Am Chem Soc 128:12090–12097
7. Guo DZ, Zhang GM, Zhang ZX, Xue ZQ, Gu ZN (2006) J Phys Chem B 110:1571–1575
8. Abou-Rachid H, Hu A, Timoshevskii V, Song Y, Lussier LS (2008) Phys Rev Lett 100:196401(4)
9. Ji W, Timoshevskii V, Guo H, Abou-Rachid H, Lussier LS (2009) Appl Phys Lett 95:021904(3)
10. Wang LX, Xu J, Zou HT, Yi CH (2010) Acta Phys Chim Sin 26:721–726
11. Wang LX, Yi CH, Zou HT, Xu J, Xu WL (2010) Chem Phys 367:120–126
12. Wei WM, Zheng RH, Tian Y, He TJ, He L, Chen DM, Liu FC (2007) Chin J Chem Phys 20:126–134
13. Kekin YU, Shańko VN, Stepanov RS (1989) Kinet Catal 30:848–854
14. Svensson M, Humbel S, Froese RDJ, Matsubara T, Sieber S, Morokuma K (1996) J Phys Chem 100:19357–19363
15. Becke AD (1993) J Chem Phys 98:5648(6)
16. Rappe AK, Casewit CJ, Colwell KS, Goddard WA, Skiff WM (1992) J Am Chem Soc 114:10024–10035
17. Ellison MD, Morris ST, Sender MR, Brigham J, Padgett NE (2007) J Phys Chem C 111:18127–18134
18. Ricca A, Bauschlicher Jr CW, Maiti A (2003) Phys Rev B 68:035433(7)
19. Liu LV, Tian WQ, Wang YA (2006) J Phys Chem B 110:1999–2005
20. Basiuk VA (2003) J Phys Chem B 107:8890–8897
21. Iafe RG, Houk KN (2008) J Org Chem 73:2679–2686
22. Brzostowska EM, Hoffmann R, Parish CA (2007) J Am Chem Soc 129:4401–4409
23. Penoni A, Palmisano G, Zhao Y, Houk KN, Volkman J, Nicholas KM (2009) J Am Chem Soc 131:653–661
24. Sun CK, Zhao HM, Li ZH (2004) Sci China B 47:373–380
25. Frisch MJ, Trucks GW, Schlegel HN, et al (2005) Gaussian 03, Revision E.01. Gaussian, Inc, Wallingford, CT
26. Guo YQ, Greenfield M, Bhattacharya A, Bernstein ER (2007) J Chem Phys 127:154301(10)
27. Saxon RP, Yoshimine M (1989) J Phys Chem 93:3130–3135
28. Eckert-Maksic M, Maskill H, Zrinski I (2001) J Chem Soc Perkin Trans 2:2147–2154
29. Cox RA (1996) Can J Chem 74:1779–1783
30. Velardez GF, Alavi S, Thompson DL (2005) J Chem Phys 123:074313(8)
31. Chakraborty D, Muller RP, Dasgupta S, Goddard WA III (2000) J Phys Chem A 104:2261–2272
32. Lewis JP, Glaesemann KR, VanOpdorp K, Voth GA (2000) J Phys Chem A 104:11384–11389
33. Kohno Y, Ueda K, Imamura A (1996) J Phys Chem 100:4701–4712
34. Zhang S, Truong NT (2001) J Phys Chem A 105:2427–2434
35. Halls MD, Schlegel HB (2002) J Phys Chem B 106:1921–1925
36. Halls MD, Raghavachari K (2005) Nano Lett 5:1861–1866
37. Xiao B, Zhao JX, Ding YH, Sun CC (2009) Sci China B 52:1969–1972